Electronic excitation in collisions of H_2^+ on He

Richard J. Furlan and Arnold Russek
Department of Physics, The University of Connecticut, Storrs, Connecticut 06269
(Received 16 May 1990; revised manuscript received 17 August 1990)

Ab initio cross sections have been calculated for electronic excitation resulting from single collisions in the keV energy range between H_2^+ initially in the ground electronic and vibrational state incident on He targets. These collisional excitation studies are based on *ab initio* calculations of the three lowest adiabatic states of the $(HeH_2)^+$ quasimolecular system and *ab initio* calculations of the nonadiabatic gradient coupling matrix elements between these three adiabatic states. With use of straight-line trajectories in the classical trajectory approximation, cross sections have been obtained for (1) charge exchange into the ground state of He and (2) collisional dissociation via electronic excitation $1\sigma_g \rightarrow 1\sigma_u$ of the H_2^+ projectile. Furthermore, with a knowledge of the diabatic structure of the $(HeH_2)^+$ energy levels, (3) the sum of the cross sections for Rydberg excitation of the He target or Rydberg excitation of the H_2^+ projectile or charge exchange into the repulsive state of H_2 was also obtained. The calculated cross sections are in reasonable agreement with available experimentally measured cross sections. The energy thresholds for these cross sections are found to be determined by excitation at level crossings between the ground electronic state and the $H_2^+(1\sigma_u)+He(1s^2)$ at $R \simeq 1.2$ a.u. and the $H_2^+(1\sigma_g)+He(1s,2l)$ at $R \simeq 0.7$ a.u.

I. INTRODUCTION

The few-electron $(HeH_2)^+$ triatomic system is sufficiently tractable as to provide a prototype confrontation between experimental and *ab initio* calculated cross sections for specific electron excitation processes. In this work, *ab initio* cross sections are obtained for electronic excitation resulting from single collisions in the keV energy range between H_2^+ projectiles initially in the ground electronic and vibrational state incident on He targets. These collisional excitation studies are based on state-of-the-art *ab initio* energy surfaces of the three lowest adiabatic states of the $(HeH_2)^+$ triatomic quasimolecular system and of the nonadiabatic coupling matrix elements between them by Furlan, Bent and Russek.[1] With these three adiabatic states, cross sections have been obtained for charge exchange, process (a) of Eq. (1), and collisional dissociation, process (b). Furthermore, with an unstanding of the diabatic structure of the $(HeH_2)^+$ energy levels described by Russek and Furlan,[2] a combined cross section has been obtained for processes (c), (d), and (e). Process (c) denotes Rydberg excitation of the target He, process (d) denotes Rydberg excitation of the H_2^+ molecular ion (which subsequently dissociates), while (e) represents charge exchange into the repulsive state of H_2. *Ab initio* calculation of the branching ratios between processes (c), (d), and (e) is beyond the scope of a three-state calculation, but the excitation processes can be qualitatively understood in terms of the diabatic level structure. In fact, without an understanding of the diabatic structure of the molecular energy surfaces, erroneous results would also have been obtained for processes (a) and (b):

$$\begin{aligned} H_2^+(1\sigma_g)+He(1s^2) &\rightarrow H_2(1\sigma_g^2)+He^+(1s) \quad \text{(a)} \\ &\rightarrow H_2^+(1\sigma_u)+He(1s^2) \quad \text{(b)} \\ &\rightarrow H_2^+(1\sigma_g)+He(1s,nl) \quad \text{(c)} \\ &\rightarrow H_2^+(n=2,l)+He(1s^2) \quad \text{(d)} \\ &\rightarrow H_2(1\sigma_g,1\sigma_u)+He^+(1s) \quad \text{(e)} . \end{aligned} \tag{1}$$

The collisional excitation calculations are described in Sec. II, along with the *ab initio* cross sections obtained for processes (a), (b), and (c)+(d)+(e) as functions of the collision energy. With the help of the diabatic level structure, the theoretical results are compared in Sec. III with experimental cross sections for collisional dissociation of the H_2^+ projectile inferred from the measurements of Alvarez, Cisneros, and Russek.[3] To make the comparison between theory and experiment, the measured angular distributions of H^+ dissociation fragments is decomposed in Sec. III into an electronically elastic component (produced by repulsive polarization forces entirely in the ground electronic state) and a component due to electronic excitation, processes (b) and (d). Dissociation produced by excitation of H_2^+ to the $1\sigma_u$ repulsive state has long been known. However, it has recently been shown that the H_2^+ can also dissociate via electronic excitation to a Rydberg state. The results of Jaecks *et al.*[4] conclusively demonstrate the existence of Rydberg excitation of the H_2^+ molecular ion, which then dissociates into $H^+ + H(n=2,l)$, a process which can also be understood in terms of the diabatic level structure. The

cross sections for these processes cannot be calculated separately, however. The best that can be accomplished within the three-state approximation is a combined cross section for Rydberg excitation of He, H_2^+, or for charge exchange into the repulsive $b\ ^3\Sigma_u(1\sigma_g, 1\sigma_u)$ state of H_2. In Sec. III, the experimental cross sections for Rydberg excitation of He obtained by Van den Bos, Winter, and DeHeer[5] and the cross section for charge exchange into the repulsive $b\ ^3\Sigma_u$ state of H_2 inferred from the measured angular distributions of Alvarez, Cisneros, and Russek[3] are compared with the calculated cross sections. Rather good agreement between theory and experiment is found, particularly in the energy dependence, in spite of the fact that the theoretical results were calculated for the incident H_2^+ molecular ion in the ground vibrational state, whereas the experimental measurements were undoubtedly obtained with the projectiles in a distribution of excited vibrational states.

Section IV discusses the results. In particular, the basic energy dependence of processes (c), (d), and (e), with an energy threshold $\simeq 1$ keV, is shown to arise from excitation at an inner level crossing at $R \simeq 0.7$ a.u. between the incident channel and a Rydberg level. The critical level crossing for processes (a) and (b) is at $R \simeq 1.2$ a.u., and gives a slightly different energy dependence, with a somewhat lower energy threshold.

II. CALCULATIONS

The energy surfaces of the three lowest adiabatic states and the nonadiabatic gradient matrix elements which couple these states were obtained *ab initio* by Furlan, Bent, and Russek[1] for the $(HeH_2)^+$ molecular system, using the *BRLJHU* (Refs. 6–9) system of programs. The procedure consists of state-averaged multiconfiguration self-consistent-field calculations, followed by a full configuration-interaction calculation. The energies E_i and coupling matrix elements $M_{ij} = \langle \Psi_i | \nabla \Psi_j \rangle$ reported in that work are here used as inputs to collisional excitation calculations, which are therefore limited to a three-state approximation. The collision calculations are based on the classical trajectory approximation, using straight-line trajectories. This approximation should be valid for total cross sections in the low-keV collision-energy regime. Two factors limit the validity of the present work in the high-keV collision-energy regime. In the first place, the nonadiabatic gradient coupling matrix elements were calculated by the *BRLJHU* programs without electron translation factors. Even more important, however, is the failure of the three-state approximation, the onset of which will be seen already in evidence at 12.5 keV collision energy. The set of coupled equations for the amplitudes of the three lowest states, obtained from the time-dependent Schrödinger equation, are solved for straight-line trajectories (see Fig. 1) from $Z = -5$ to $+5$. The input values for the energy differences $E_i - E_j$ and coupling matrix elements M_{ij} were obtained by interpolating the *ab initio* values in Tables 3 and 6 of Ref. 1, using an interpolation method similar to that described by Akima,[10] which is part of the *SAS/GRAPH* (Ref. 11) software plotting package.

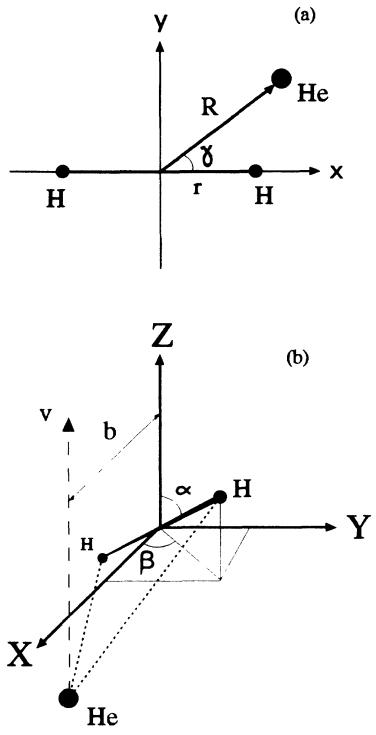

FIG. 1. Collision geometry. (a) shows the molecular geometry in the molecule-centered coordinate system $[(x,y,z)$ or $(r,R,\gamma)]$, while (b) shows the trajectory geometry in a space-fixed coordinate system (X,Y,Z).

The set of coupled integral equations were integrated numerically with a simple program that runs on a personal computer. The solutions thus obtained *would* be valid provided that the three lowest adiabatic levels did not interact with any others. However, this important condition is not satisfied. Figure 2(a) shows the three lowest

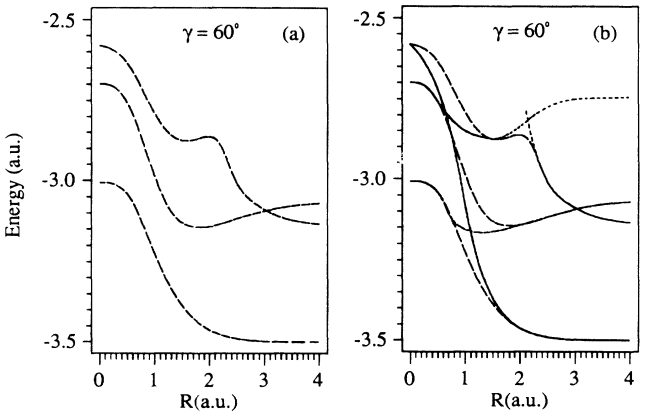

FIG. 2. Adiabatic and diabatic energy levels. (a) shows the three lowest adiabatic energy levels obtained by Furlan, Bent, and Russek (Ref. 1) for the case $r = 2.0$ a.u. and $\gamma = 60°$, while (b) shows these same three levels along with the diabatic energy levels obtained by Russek and Furlan (Ref. 2). In (b), the solid curves are the diabatic levels, the dashed curves are the adiabatic levels, and the dotted curve has only been interpolated from the known value at $R = \infty$.

adiabatic levels as obtained by Furlan, Bent, and Russek for the case $r=2$ a.u. and $\gamma=60°$, while Fig. 2(b) shows these same adiabatic energy levels along with the diabatic energies obtained by Russek and Furlan.[2] It is seen that the third adiabatic state interacts at $R\simeq 2$ a.u. with a highly excited level rapidly decreasing in energy from $R=0$. This same behavior was found at all angles γ at approximately the same value of R. It is expected that the system behavior at this avoided crossing will be predominantly *diabatic*. It is improbable that a diffuse electron in a Rydberg orbit (which characterizes Ψ_3 for $R<2$ a.u.) will quickly collapse into a tightly bound $1\sigma_g$ orbit tucked between the two protons, during the short time it takes to pass through the interaction region in a keV energy collision. For this reason, the behavior of the third level at $R\simeq 2$ a.u. has been taken to be completely diabatic, an ansatz which was incorporated into the collision calculations by inserting a flag in the integration program at $R=2.2$ on the outgoing portion of the trajectory: $Z=+(2.2^2-b^2)^{1/2}$, where b is the impact parameter. The amplitude a_3 at this point was stored as the final amplitude of the residual channel $a_r(+5)$, and a_3 was then reset to zero since the highly excited diabatic state, which the adiabatic state Ψ_3 becomes, cannot have been populated under the given initial conditions. The final population of the adiabatic state Ψ_3 at $R=\infty$ results from the branching ratio at the avoided crossing between levels 2 and 3 at $R\simeq 3$ a.u.

The state shown as the dotted curve of Fig. 2(b) has the diabatic character $H_2^+(1\sigma_g)+He(1s,2l)$. However, it interacts with other Rydberg levels of He as well as with the several $n=2$ Rydberg levels of H_2^+ and with the $H_2(1\sigma_g,1\sigma_u)+He^+(1s)$ level, which describes charge exchange into the repulsive state of H_2. This latter can be seen as the fourth level in Fig. 3. The Rydberg levels of the projectile molecular ion $H_2^+(n=2,l)+He(1s^2)$ are still higher in energy and were not obtained with sufficient accuracy to be shown. They do, however, intersect the dotted diabatic curve of Figs. 2 and 3, lying approximately 2 eV below that curve at $R=\infty$ when $r=2$ a.u., and lie even lower when $r>2$. Unlike the Rydberg level crossing at $R\simeq 2$, which is expected to be predominantly diabatic, the crossings between the Rydberg level and the $H_2(1\sigma_g,1\sigma_u)+He^+(1s)$ and $H_2^+(n=2,l)+He(1s^2)$ states should have significant branching ratios. Although a diffuse $n=2$ electron on He was considered unlikely to fall into a tightly bound and localized $1\sigma_g$ orbit, it can easily fall into a $1\sigma_u$ orbit or $n=2$ Rydberg orbit on H_2^+. In fact, to the extent that the H_2 molecule can be considered to resemble a distorted He atom, the $1\sigma_u$ orbital and the $n=2$ Rydberg orbitals of H_2 are the $2p$ and $2s$ orbitals of the distorted He. Thus capture from a $2p$ orbit of He into the $1\sigma_u$ orbit of H_2 is quasiresonant. In any event, the cross section denoted by σ_r is the totality of cross sections to all Rydberg levels on He plus the $n=2$ Rydberg levels on H_2^+ plus the cross section for charge exchange into the repulsive state of H_2.

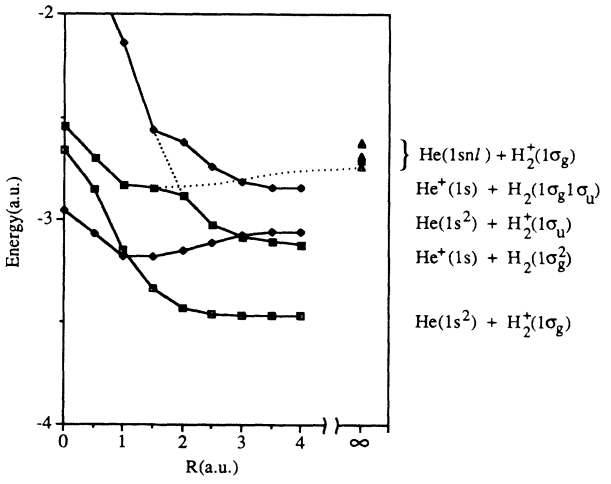

FIG. 3. The lowest four adiabatic levels for the case $r=2.0$ a.u. and $\gamma=90°$. The fourth level, although calculated *ab initio*, was not included in the state averaging, and is therefore not of the same quality as the first three. Moreover, the final configuration-interaction calculation could not be completed in this case. The level diagram is shown here just to demonstrate the diabatic crossing between the Rydberg level and the $He^+(1s)+H_2(1\sigma_g,1\sigma_u)$ level. The dotted curves indicate the diabatic levels.

The net result of the solution of the coupled equations for the amplitudes incorporating the ansatz just described is a set of probabilities for four exit channels: the elastic channel P_{el}, the charge-exchange channel P_x [process (a) of Eq. (1)], the dissociation channel due to the $1\sigma_g\rightarrow 1\sigma_u$ electronic transition in H_2^+ (often called predissociation) P_d [process (b)], and the residual excitation channel P_r [processes (c)+(d)+(e)]. These probabilities are given by

$$\begin{aligned} P_{el}&=|a_1(+Z_0)|^2\ ,\\ P_x&=|a_2(+Z_0)|^2\ ,\\ P_d&=|a_3(+Z_0)|^2\ ,\\ P_r&=|a_r(+Z_0)|^2\\ &=P_{Ry}(He)+P_{Ry}(H^++H(n=2))+P_{xd}\ . \end{aligned} \tag{2}$$

They are functions of impact parameter b and the orientation angles α and β of the target molecule. The cross sections for these processes are obtained by integrating the final probabilities over all impacts in the target plane and averaging over molecular orientation angles. The final cross sections as functions of collision energy in the laboratory frame for the processes obtained in this work are shown in Fig. 4.

III. RESULTS AND COMPARISON WITH EXPERIMENT

A. Rydberg excitation of the He target

The cross section σ_r represents the sum of the cross sections to the $n=2$ Rydberg state of He plus any state which interacts with it. This includes Rydberg states with $n>2$, Rydberg states of H_2^+ plus one important valence channel: charge exchange to the $b\ ^3\Sigma_u$ repulsive state of H_2. Thus

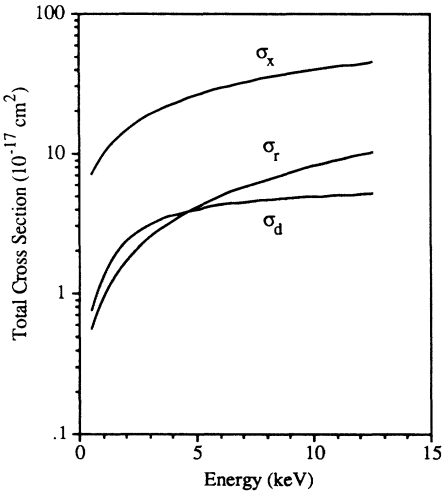

FIG. 4. *Ab initio* cross sections obtained in this work for σ_d, σ_x, and σ_r. These denote direct dissociation of H_2^+ via $1\sigma_g \rightarrow 1\sigma_u$ electronic excitation, charge exchange into the ground state of H_2, and a residual excitation cross section $\sigma_r = \sigma_{Ry} + \sigma_{xd}$ as described in the text.

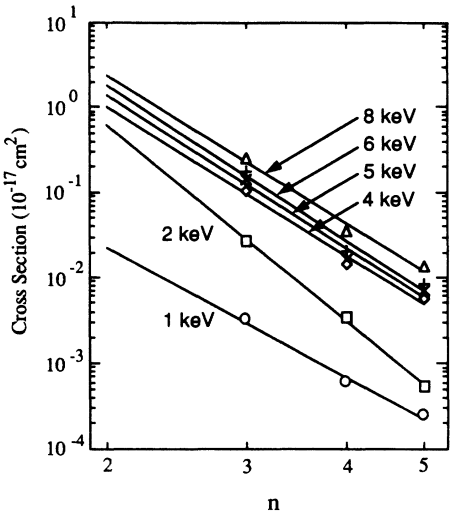

FIG. 6. Cross sections for Rydberg excitation of He obtained by Van den Bos *et al.* for $n > 2$ on a log-log plot. The lines are least-squares fits to the experimental data and are extrapolated to $n = 2$.

$$\sigma_r = \sigma_{Ry}(\mathrm{He}) + \sigma_{Ry}(H_2^+) + \sigma_{xd} \ . \tag{3}$$

The calculated cross sections for σ_r are compared in Fig. 5 with the experimental values obtained by Van den Bos *et al.*[4] for excitation to all Rydberg states $n > 2$ plus our estimate for the $n = 2$ cross section obtained by extrapolating their experimental values for $n > 2$ to $n = 2$. (Van den Bos *et al.* could not measure excitation to the $n = 2$ level since their spectrometry was limited to the visible region.) The extrapolation, shown in Fig. 6, is expected to give an underestimate of the cross section to $n = 2$ and hence an underestimate of the total Rydberg cross section to all n, σ_{Ry}(He). A comparison between the theoretical prediction for σ_r and the extrapolated experimental values for σ_{Ry}(He) suggests that at the avoided crossings between the He Rydberg level and the repulsive H_2 level, on the one hand, and the H_2^+ Rydberg level, on the other, the probability is only 0.2 that the collision system will remain in the He Rydberg channel. However, Fig. 5 shows that the predicted energy dependence of σ_r closely matches the experimental σ_{Ry}(He). As would be expected, the principal energy dependence of each of the cross sections under discussion is the energy dependence of getting up to Ψ_r in the first place. This point will be discussed further in Sec. IV.

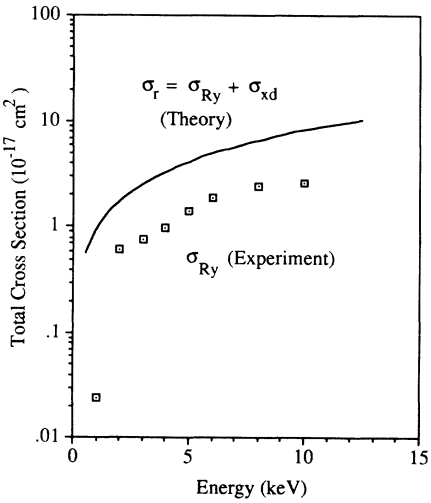

FIG. 5. Comparison of the calculated σ_r of Fig. 4 with the sum of the He Rydberg excitation cross sections measured by Van den Bos *et al.* (Ref. 4) for $n > 2$, plus an $n = 2$ contribution extrapolated from the measured cross sections (see Fig. 6).

B. Dissociation cross section

Electronic excitation of the H_2^+ projectile from the $1\sigma_g$ ground state to the repulsive $1\sigma_u$ state or to a Rydberg state both result in dissociation to H^+ and H fragments, which separate with a relative velocity corresponding to dissociation energies of approximately 12 and 20 eV in the H_2^+ frame when the H-H separation $r = 2$ a.u. The dissociation energy rapidly decreases as r increases. Experimentally, the dissociation cross section is measured by detecting the protons, which are found in a broad angular distribution with respect to the incident beam direction, arising from the distribution of molecular orientations at the time of dissociation. However, electronic excitation is not the only collisional mechanism which causes dissociation. Dissociation can also occur entirely within the electronic ground state (the electronically elastic channel) caused by impulsive momentum transfer to the vibrational degree of freedom from polarization induced forces. This mechanism was first suggested by Russek[12] and verified experimentally by Schopman and co-workers,[13] Anderson and Swan,[14] and Anderson.[15] The cross section $\sigma_d(1\sigma_u)$ as defined here refers only to

the dissociation cross section arising from the $1\sigma g \rightarrow 1\sigma_u$ transition. This work has not been able to address dissociation caused by direct excitation of H_2^+ to a molecular Rydberg level. To make a comparison, the cross section due to electronic excitation must first be separated from the overall dissociation cross section. This can be accomplished (for low vibrational states) because of the different regimes of dissociation energies involved in the two very different dissociation mechanisms. Dissociation by polarization induced forces results only in small dissociation energies, with the consequence that the protons thus produced will be detected at small angles with respect to the beam direction. On the other hand, electronic excitation to the repulsive state produces large dissociation energies, and protons arising from this process will be found at larger angles. Figure 7 shows the angular distributions for H^+ found by Alvarez, Cisneros, and Russek[3] produced by collisions with He at 2 keV in the laboratory frame. The distribution consists of two components indicated by the dashed lines, which give

$$\frac{d\sigma}{d\omega} \simeq 4.0\times10^{-13}e^{-69.70\theta}+5.0\times10^{-15}e^{-22.42\theta}\ , \tag{4}$$

where cross sections are given in units of 10^{-17} cm^2 and angles are measured in radians. The first component is here identified with polarization-induced dissociation (PID), while the second is attributed to electronic excitation. The total dissociation cross sections are given by

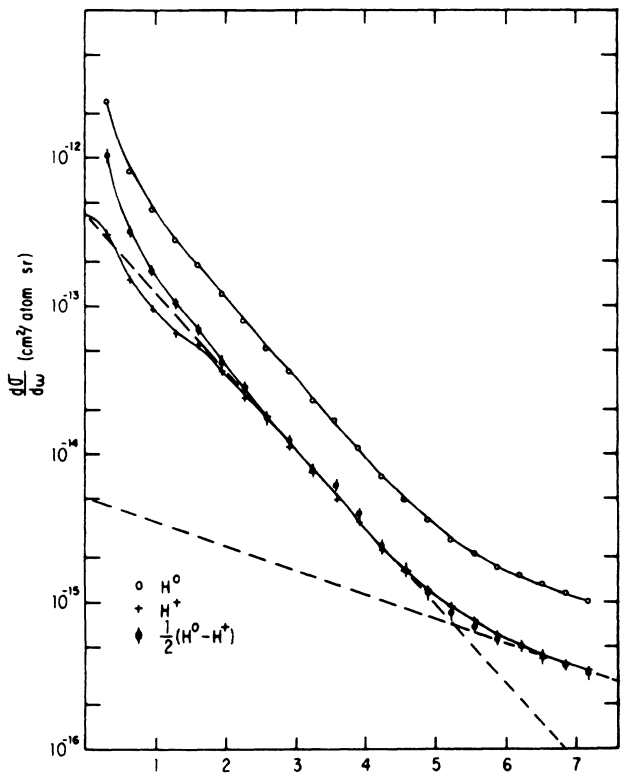

FIG. 7. Absolute angular distributions of dissociation fragments measured by Alvarez, Cisneros, and Russek (Ref. 3) for collisions of H_2^+ on He at 2-keV collision energy. The dashed straight lines show the decomposition of this distribution to yield the approximation represented by Eq. (4) of the text.

$$\sigma_{\rm PID}(1\sigma_g)+\sigma_d(\text{el.ex.})=\int_0^{\pi}\frac{d\sigma}{d\omega}2\pi\sin\theta\,d\theta\ . \tag{5}$$

The integrals arising in (5) are standard, and for $a\pi \gg 1$ the results are quite simple:

$$\int_0^{\pi} e^{-a\theta}\sin\theta\,d\theta \simeq \frac{1}{1+a^2} \quad \text{for } a\pi \gg 1\ . \tag{6}$$

As a consequence, that component of the direct dissociation cross section here identified as the electronically elastic dissociation cross section at 2 keV is found to be

$$\sigma_{\rm PID}(1\sigma_g)=51.8\times10^{-17}\ \text{cm}^2\ \ (\text{expt.})\ . \tag{7}$$

The experimental cross section for dissociation here identified as being due to electronic excitation can be compared with the 2 keV results shown in Fig. 4:

$$\begin{aligned}\sigma_d(\text{el.ex.})&=6.2\times10^{-17}\ \text{cm}^2\ \ (\text{expt.})\ ,\\ \sigma_d(1\sigma_u)&=2.4\times10^{-17}\ \text{cm}^2\ \ (\text{theor.})\ .\end{aligned} \tag{8}$$

The difference between the experimental and theoretical results in (8) does not necessarily represent a discrepancy between theory and experiment. The theoretical cross section was calculated only for excitation to the $1\sigma_u$ state when $r=2$ a.u., representing the ground vibrational state for the H_2^+. On the other hand, the experimental cross sections were unquestionably obtained with the projectile H_2^+ in a distribution of high vibrational states and include excitation to the several Rydberg levels of H_2^+ as well as the $1\sigma_u$ level. For collision energies of 1 keV, Lindsay, Yousif, and Latimer[16] obtained a ratio $\sigma_d(v=5)/\sigma_d(v=0)=1.7$, while Gibson, Los, and Schopman[17] obtained the value 2.1 for this same ratio at 3-keV collision energy. Thus theory and experiment are not far apart for incident H_2^+ in the $v=5$ vibrational state, if the dissociation of H_2^+ is equally divided between $1\sigma_u$ and Rydberg excitation of the H_2^+. The discrepancy would be approximately a factor of 2.6 in the extreme case for which H_2^+ was in the ground vibrational state and Rydberg excitation of H_2^+ was negligible.

Looked at in a different way, this rather good agreement between theory and experiment for the component of the dissociation cross section due to electronic excitation lends strong support to the identification of the two components of the dissociation cross section, and provides further verification of the polarization induced dissociation process.

C. Capture into the repulsive state of H_2

Alvarez, Cisneros, and Russek also presented an angular distribution at 2-keV collision energy for neutral H produced by electron capture into the repulsive $b\,^3\Sigma_u(1\sigma_g,1\sigma_u)$ state of H_2. Because neutral H is produced by direct dissociation as well as by electron capture into the repulsive state, the angular distribution leading to σ_{xd} was obtained by Alvarez, Cisneros, and Russek by subtracting the distribution of H^+ from that of H to remove those neutral H fragments arising from dissociation of H_2^+. The residual H distribution, which arose solely from the dissociation of H_2, was then divided by 2, since

each such dissociation produces two H fragments. This angular distribution is also shown in Fig. 7. It has a high-energy tail described by

$$\frac{d\sigma_{xd}}{d\omega} \simeq 5\times 10^{-15} e^{-22.42\theta}, \tag{9a}$$

from which it follows that

$$\sigma_{xd}(2\text{ keV}) = 6.2\times 10^{-17}\text{ cm}^2\text{ (expt.)}. \tag{9b}$$

On the other hand, from Fig. 4 it is seen that

$$\sigma_r(2\text{ keV}) = \sigma_{\text{Ry}}(\text{He}) + \sigma_{\text{Ry}}(H_2^+) + \sigma_{xd} = 1.8\times 10^{-17}\text{ cm}^2\text{ (theor.)}. \tag{10}$$

Allowing for an approximate contribution of 0.5×10^{-17} cm^2 for $\sigma_{\text{Ry}}(\text{He}) + \sigma_{\text{Ry}}(H_2^+)$ to the overall value of σ_r leaves a theoretical prediction of

$$\sigma_{xd}(2\text{ keV}) \simeq 1.3\times 10^{-17}\text{ cm}^2\text{ (theor.)}. \tag{11}$$

As in the case of direct dissociation, the factor-of-5 discrepancy between theory and experiment is most likely due to the fact that the theoretical cross section was calculated for an initial ground vibrational state, whereas the experimental results were almost certainly obtained with H_2^+ in a distribution of high vibrational states. At this time, it is not known how the vibrational state affects the electron-capture cross section.

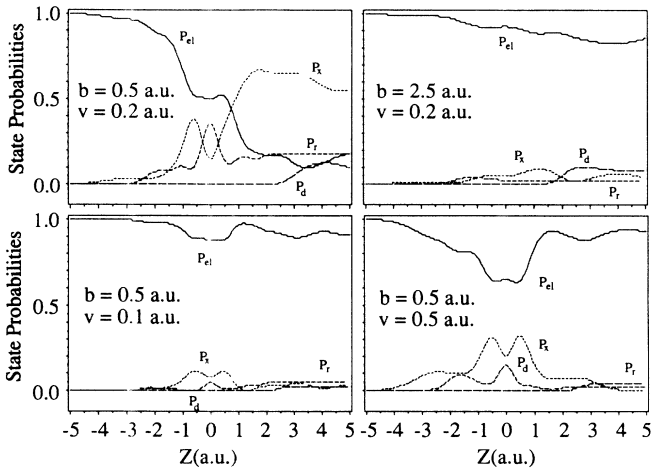

FIG. 8. State probabilities as functions of position Z along the collision trajectory obtained for the case $r=2.0$ a.u., $\alpha=90°$, and $\beta=30°$ for four different impact conditions. The upper pair of figures is for the case $v=0.2$ a.u. ($E_{\text{inc}}=2.0$ keV), an incident energy above the threshold for nonadiabatic excitation. At impact parameter $b=0.5$ a.u., inside both level crossings, substantial excitation is seen. For larger impact parameters, outside both level crossings, the collision is nearly adiabatic. The lower pair of figures illustrates the velocity dependence of excitation at an impact parameter $b=0.5$ a.u. At $v=0.1$ a.u., corresponding to incident energy of 0.5 keV, the collision is completely adiabatic. On the other hand, at $v=0.5$ a.u. (12.5 keV), the collision is seen to be more nearly diabatic.

IV. DISCUSSION

In summary, the theoretical predictions for the several excitation cross sections presented here and the available experimental measurements compare favorably, despite the fact that in no case did theory and experiment refer exactly to the same process. The threshold energy dependences of the excitation cross sections σ_{Ry} and σ_{xd} are both due to the energy dependence of excitation from the ground electronic state into the Rydberg channel at the inner crossing at $R\simeq 0.7$ a.u. The physics of the situation can be seen in Fig. 8, which shows the evolution of the state probabilities for several different collision geometries. The upper pair of figures illustrates the impact parameter dependence of electronic excitation at a collision velocity $v=0.2$ a.u. (corresponding to 2.0-keV beam energy in the laboratory), a velocity above the threshold for nonadiabatic excitation. For impact parameter $b=0.5$ a.u., inside both critical crossing radii, significant electronic excitation is seen. Well outside the crossing radii, at $b=2.5$, no significant excitation takes place. The lower pair of figures shows the velocity dependence of electronic excitation at fixed impact parameter $b=0.5$ a.u., for which significant excitation was seen to be possible. At $v=0.1$ a.u., corresponding to 0.5 keV, the collision is seen to be adiabatic; at $v=0.2$ a.u. (2.0 keV), nonadiabatic excitation was seen (upper left figure), and, finally, at $v=0.5$ a.u. (12.5-keV laboratory energy), the collision exhibits partially *diabatic* behavior, as evidenced by the fact that the time evolution on the outgoing half of the trajectory reverses the changes which occurred on the incoming half of the trajectory. Indeed, one can follow the diabatic component of the quasimolecular state through the collision trajectory. For large values of R, this diabatic state is the lowest adiabatic state; for intermediate values of R, it has a substantial component of the second adiabatic state; for small values of R, the second adiabatic state gives way to the third adiabatic state. However, it should be noted that at 12.5 keV, the collision is not completely diabatic. It appears to be partway between adiabatic and diabatic, but that is an artifact of the small basis set here used. At still higher collision energies, the three-state approximation appears to approach adiabaticity. This demonstrates a failure of the quasimolecular approach, since the high-energy limit must, of course, be atomic and not adiabatic. It is noteworthy that there is no energy at which the collision is fully diabatic. The onset of diabatic behavior occurs as the quasimolecular approximation (with a limited basis set) breaks down. It should also be noted that this partial diabatic behavior is seen only for $\alpha=90°$, for which the collision geometry has reflection symmetry in the plane $Z=0$. For other values of α, the outgoing half of the trajectory is not the mirror image of the incoming half, and the electronic behavior is even less diabatic. In this regard, collisions involving molecules differ from collisions which involve atoms only.

Figures 9 and 10 illustrate the orientation dependence of electronic excitation. Excitation is found to be more likely when the molecular axis is aligned parallel to the collision trajectory. Figure 10 also illustrates the impact

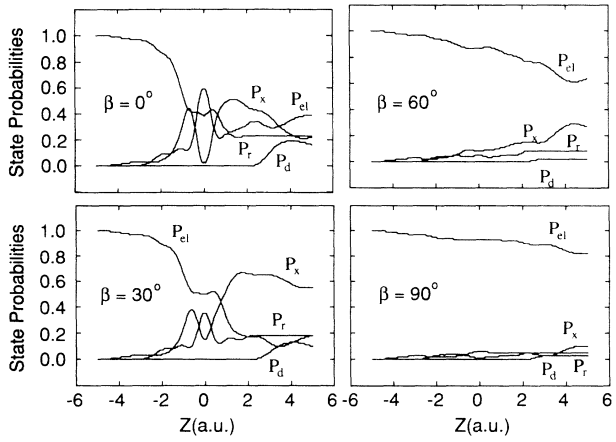

FIG. 9. State probabilities as functions of Z for $r=2.0$ a.u. and impact parameter $b=0.5$ obtained for four different molecular azimuthal orientations β. All cases are for $\alpha=90°$ (molecular axis perpendicular to the collision trajectory).

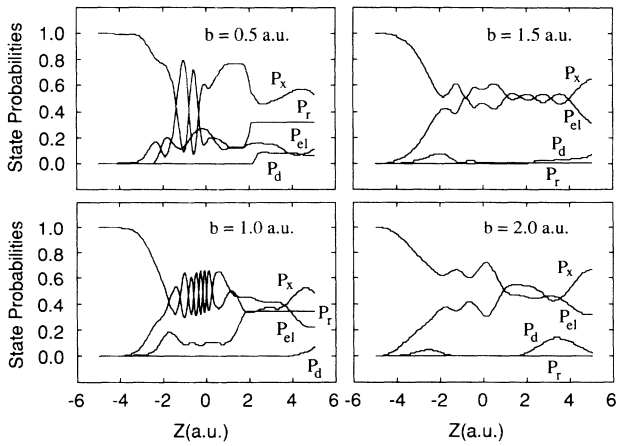

FIG. 10. State probabilities as functions of Z for $r=2.0$ a.u. and $\alpha=0°$ (molecular axis oriented parallel to the collision trajectory). In this case, the results are the same for all values of β. Results are shown for four values of impact parameter. It is seen that P_r falls off very rapidly for $b>1.0$, while P_x falls off more slowly. This is to be expected, since excitation to Ψ_r occurs at the inner crossing at $R\simeq 0.7$ a.u., while excitation to Ψ_x occurs at a larger value of R.

parameter dependences of the several collisional excitation processes. The combined processes lumped together in P_r fall off rapidly with impact parameter beyond $b=1.0$, as would be expected from a level crossing at $R\simeq 0.7$ a.u. The exchange process, on the other hand, arises from a crossing which, depending on the value of γ (see Fig. 1), varies from $R\simeq 1.2$–2.0 a.u. As might be expected, this cross section falls off rather slowly with increasing impact parameter, dropping off rapidly between $R=2.0$ and 2.5 a.u.

ACKNOWLEDGMENTS

The authors would like to thank Byron Lengsfield and David Yarkony for permission to use the BRLJHU system of programs. The work was supported in part by the National Science Foundation, under Grant Nos. PHY-85-07736 and PHY-86-45049. Molecular calculations were carried out at the Cornell National Supercomputer Facility, a resource of the Center for Theory and Simulations in Science and Engineering, which receives major funding from the National Science Foundation and IBM Corporation, with additional support from New York State and members of the Corporate Research Institute.

[1]R. J. Furlan, G. Bent, and A. Russek, J. Chem. Phys. **93**, 6676 (1990).
[2]A. Russek and R. J. Furlan, Phys. Rev. A **39**, 5034 (1989).
[3]I. Alvarez, C. Cisneros, and A. Russek, Phys. Rev. A **23**, 2340 (1981).
[4]D. H. Jaecks, O. Yenen, L. Wiese, and D. Calabrese, Phys. Rev. A **41**, 5934 (1990).
[5]J. Van den Bos, G. Winter, and F. J. De Heer, Physica **44**, 143 (1969).
[6]R. N. Diffender and D. R. Yarkony, J. Phys. Chem. **86**, 5098 (1980).
[7]B. H. Lengsfield III, P. Saxe, and D. R. Yarkony, J. Chem. Phys. **81**, 4549 (1984).
[8]P. Saxe, B. H. Lengsfield III, and D. R. Yarkony, Chem. Phys. Lett. **113**, 159 (1985).
[9]M. Page, P. Saxe, G. F. Adams, and B. H. Lengsfield III, J. Chem. Phys. **81**, 434 (1984).
[10]H. Akima, ACM Trans. Math. Software **4**, 148 (1978).
[11]Statistical Analysis System (SAS) Institute Inc. *SAS/GRAPH* User's Guide, Version 5, 1985.
[12]A. Russek, Physica **48**, 165 (1970).
[13]J. Schopman and J. Los, Physica **48**, 190 (1970); J. Schopman, J. Los, and J. Maas, *ibid.* **51**, 113 (1971); J. Schopman and J. Los, *ibid.* **51**, 132 (1971).
[14]S. J. Anderson and J. B. Swan, Phys. Lett. **48A**, 435 (1974).
[15]S. J. Anderson, J. Chem. Phys. **60**, 3278 (1974).
[16]B. G. Lindsay, F. B. Yousif, and C. J. Latimer, J. Phys. B **21**, 2593 (1988).
[17]D. K. Gibson, J. Los, and J. Schopman, Physica **40**, 385 (1968).